



# Dynamic response of offshore triceratops with elliptical buoyant legs

R. Nagavinothini<sup>1</sup> · Srinivasan Chandrasekaran<sup>2</sup>

Received: 9 February 2020 / Accepted: 24 April 2020 / Published online: 4 May 2020  
© Springer Nature Switzerland AG 2020

## Abstract

Oil and gas exploration in ultra-deepwaters necessitates innovative geometric forms for offshore steel structures. Offshore triceratops is one of a new steel compliant structures found suitable for ultra-deepwater applications. It consists of three buoyant legs attached to the deck by ball joints, which partially isolate the deck from the buoyant legs and constitute the novelty. The present study discusses a detailed numerical analysis of triceratops with buoyant legs of elliptical cross section. The focus is to assess the hydrodynamic diffraction characteristics of the platform caused by the change in cross section of buoyant legs from a conventional tubular one to the elliptical ones. Three elliptical sections with varying eccentricities are considered in the dynamic analyses to assess the response behavior of triceratops under regular waves. The results showed an increase in the total force in the buoyant legs in sway degree of freedom with the increase in the eccentricity of the cross section. Besides, reduced transverse vibrations and increased stability are also observed in both the deck and elliptical buoyant legs. Based on the numerical results, it is recommended that elliptical buoyant legs with eccentricity close to 2 are highly suitable for offshore triceratops in ultra-deepwaters.

**Keywords** Buoyant legs · Elliptical section · Wave loads · Triceratops · Offshore steel structures · Ball joints

## Introduction

Offshore oil drilling and production platforms are heading toward ultra-deepwaters in the recent past. A severe combination of environmental and accidental loads in a marine environment demands an adaptive structural form to alleviate the loads effectively. Triceratops is one of the recent and innovative structural forms of offshore compliant structures, which is found more adaptable to ultra-deepwaters [3, 4, 10]. Triceratops consists of three buoyant legs connected to the deck by ball joints [16]. These ball joints restrain the transfer of rotation but enable the translation between the deck and the buoyant legs. Partial isolation of the deck from the buoyant legs reduces the response of the deck under the wave loads. Buoyant legs are position-restrained by a set

of taut-moored tethers, making it stiff in the vertical plane, while offers compliancy in the horizontal plane. Detailed response analyses of triceratops validate its capacity to withstand wave, wind, current, and ice loads in ultra-deepwaters [3, 5, 12]. Buoyant legs of the circular cross section were designed as stiffened cylindrical shell structures similar to that of a hull of a spar platform. As the wave forces dominate the response of buoyant legs, investigations need to be carried out to reduce the total force acting on the legs. Marginal modifications made on the buoyant legs by interconnecting them to the central moon pool with stiffeners showed a significant reduction in the response, but with an increase in the forces attracted by the legs [2]. As triceratops is in the developmental stage, detailed analyses of this innovative steel platform with different structural modifications may aid in improving the operational advantages of the platform. In this context, the present study aims to assess the dynamic response of offshore triceratops with elliptical buoyant legs.

Large structures with elliptical cross section are currently under consideration for use in offshore oil drilling and production platforms. With the inclusion of an elliptical section in the European Norm 10210 [1, 11], the use of steel elliptical hollow sections is becoming popular due to their viable applications. However, the use of the elliptical steel section

✉ Srinivasan Chandrasekaran  
drsekaran@iitm.ac.in

R. Nagavinothini  
vino.civil35@gmail.com

<sup>1</sup> Department of Structures for Engineering and Architecture, University of Naples Federico II, Naples, Italy

<sup>2</sup> Department of Ocean Engineering, Indian Institute of Technology Madras, Chennai, India

in offshore structures is very scarce. Several studies reported an estimate of wave forces on elliptical cylinders using linear diffraction theory [17, 18]. They showed that the total wave force on elliptical cylinders depends upon the wave incident angle and phase difference [6, 15]. However, in the case of an array of elliptical cylinders, complex hydrodynamics affects the total response of the structure significantly. They induce sway force even under unidirectional waves, acting parallel to the longitudinal axis of the ellipse [7, 8]. Concerning buckling behavior, elliptical shells with moderate to high eccentricity ( $a/b \geq 2$ ) showed a higher ultimate load capacity in comparison with their buckling load capacity. It is because elliptical sections possess a stable, post-buckling behavior than that of circular cylindrical shells [13]. Numerical models of offshore triceratops with circular and elliptical buoyant legs are developed in Ansys at 2400 m water depth. The time response analysis is carried out under different sea states to assess the response of triceratops with elliptical buoyant legs. The response is also compared with the response of triceratops with cylindrical buoyant legs. Besides, detailed studies are carried out to investigate the effect of the wave-heading angle on the response of the deck with elliptical buoyant legs of different eccentricity.

## Offshore triceratops for ultra-deepwaters

The conceptual model of triceratops is shown in Fig. 1. As triceratops is in the developmental stage, the model suitable for ultra-deepwater applications is developed based on the dimensions of Perdido Spar, which is commissioned in the Gulf of Mexico at 2438 m water depth [9]. The geometric properties of the triceratops with cylindrical buoyant legs are listed in Table 1. Structural characteristics

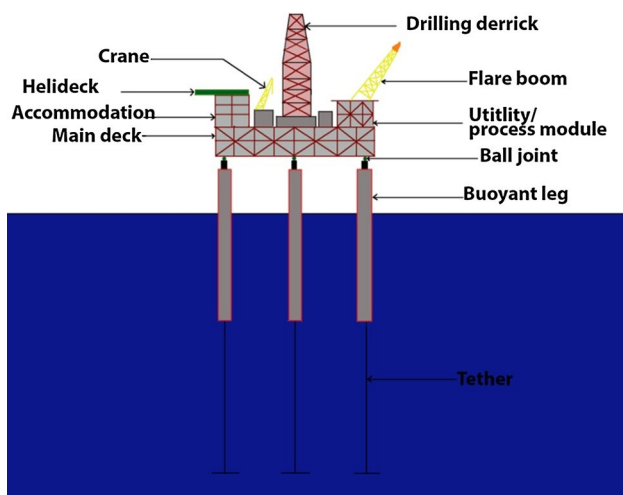


Fig. 1 Conceptual model of triceratops

**Table 1** Details of triceratops with circular buoyant leg

Description	Unit	Quantity
Water depth	m	2400
Unit weight of material	kg/m <sup>3</sup>	7850
Unit weight of seawater	kg/m <sup>3</sup>	1025
<i>Geometric details</i>		
Diameter of leg	M	15
c/c Distance between the buoyant legs	M	61.77
Freeboard	M	20.24
Draft	M	154
Tether length	M	2246
Vertical center of gravity of buoyant leg	M	-112.74
Metacentric height	M	35.83
<i>Load details</i>		
Self-weight + payload	MN	562.42
Buoyancy force	MN	820.93
Total tether force	MN	258.49
<i>Structural properties</i>		
Area of deck	m <sup>2</sup>	3933
Area of tether	m <sup>2</sup>	2.36
Stiffness of tethers	GN/m	0.22

such as total height, the height of the buoyant legs, and the topside weight of the triceratops are kept similar to that of a Spar platform. The overall buoyancy of the Spar hull is equally distributed to the three buoyant legs of a diameter of 15 m. The shape of the deck is chosen to be an equilateral triangle of length 95.0 m to ensure symmetric distribution of loads from the topside to the buoyant legs. Each buoyant leg is position-restrained by a set of three tethers, whose initial pretension is about 28 MN. The topside of the platform is designed as an integrated truss deck system comprising three decks, namely cellar, main, and the top deck. While the main deck is designed as a truss-type system, cellar and the top decks are designed with a beam-panel arrangement. Topside is also provided with the diagonal members connecting different floor levels, to resist wind loads. The preliminary design of the topside is carried out based on the bending moments developed on the respective structural components. Cylindrical buoyant legs of height 174.0 m are designed as orthogonally stiffened cylindrical shells for the intermediate environmental conditions that prevail in the Gulf of Mexico (Significant wave height = 7.9 m, peak period = 9.1 s). Each buoyant leg is designed with 70 numbers of longitudinal stiffeners along with ring stiffeners at 3.0-m center-to-center distance. Heavy ring frames are provided at the ends of the buoyant legs to improve stability. The cylindrical shell structure is also checked against buckling as per codal requirements [14], and the detailed design is reported by Chandrasekaran and Nagavinothini [3, 4].

### Cross section of buoyant legs

The circular cross section was used in the preliminary design, foreseeing the fabrication difficulties in other shapes. Due to the recent advancements, elliptical sections are currently under consideration for use in the large offshore oil drilling and production platforms. Due to its viable applications, elliptical sections are also included in the European Norm 10210. Further, elliptical shells have higher ultimate load carrying capacity and stable post-buckling behavior. In the present study, elliptical buoyant legs with different eccentricities ( $a/b$ ), as shown in Fig. 2, are considered to investigate the suitability of elliptical buoyant legs. The area of the elliptical cross section is maintained as same as that of the circular ones of diameter 15.0 m. It is required to ensure equal buoyancy of the platform under all the cases considered for the study. Details of the elliptical cross section, discussed in the study, are listed in Table 2.

### Numerical model

Numerical investigations are carried out of offshore triceratops with buoyant legs of elliptical cross section. The shape with different eccentricities is studied as parametric variations. A detailed numerical model is developed in Ansys, as shown in Fig. 3. Each of the buoyant legs and the deck is modeled as separate entities with the corresponding center of gravity and point mass. Topside along with three decks and the buoyant legs are modeled using plate elements. Wave forces acting on the buoyant legs are calculated using diffraction theory. Deck and the buoyant legs are mutually connected using ball joints that restrict the transfer of rotation

**Table 2** Dimensions of buoyant leg

Cross section	Eccentricity ( $a/b$ )	Semi-major axis, $a$ (m)	Semi-minor axis, $b$ (m)
Circular	1	7.5	7.5
Ellipse 1	1.5	9.186	6.124
Ellipse 2	2	10.567	5.263
Ellipse 3	2.5	11.859	4.743

but allow the transfer of translation between them. Subsequently, buoyant legs are anchored to the sea bed using taut-moored tethers, which are modeled as linear cables. Stiffness and the unstretched length of tethers are defined based on their geometric and material properties. It can be considered as a simple tension-only spring, where the cable tension is proportional to its stiffness. Under the action of wave loads, the cable tension varies to the force exerted on the buoyant legs. Buoyant legs are then meshed using quadrilateral plate elements with four nodes to enhance the accuracy in the finite element analyses. As these elements are capable of generating both hydrostatic force and pressure, they are found to be more appropriate. The deck is meshed using triangular and quadrilateral plate elements. Program-controlled optimum meshing is adopted to arrive at the proper meshing by following mesh quality checks to ensure accuracy in the hydrodynamic properties of the structure. Figure 4 shows the plan view of triceratops with elliptical buoyant legs.

Based on the fluid potential theory, a three-dimensional panel method is used to analyze the hydrodynamic behavior of the platform. A series of diffraction panels represent the surface of the buoyant legs. The linear superposition

**Fig. 2** Cross section of buoyant legs

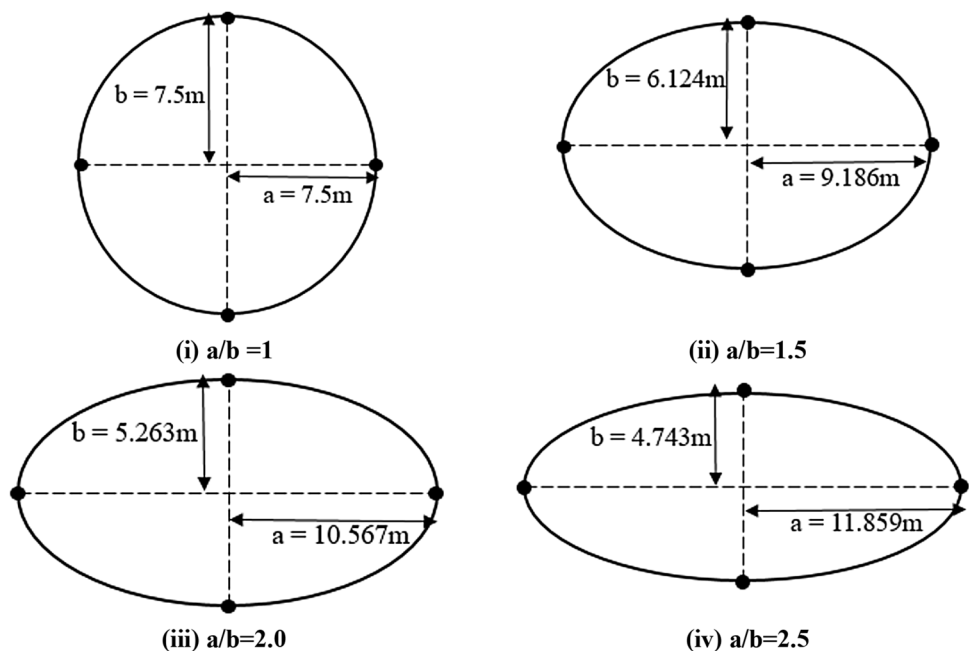


**Fig. 3** Numerical model of off-shore triceratops with circular and elliptical buoyant legs

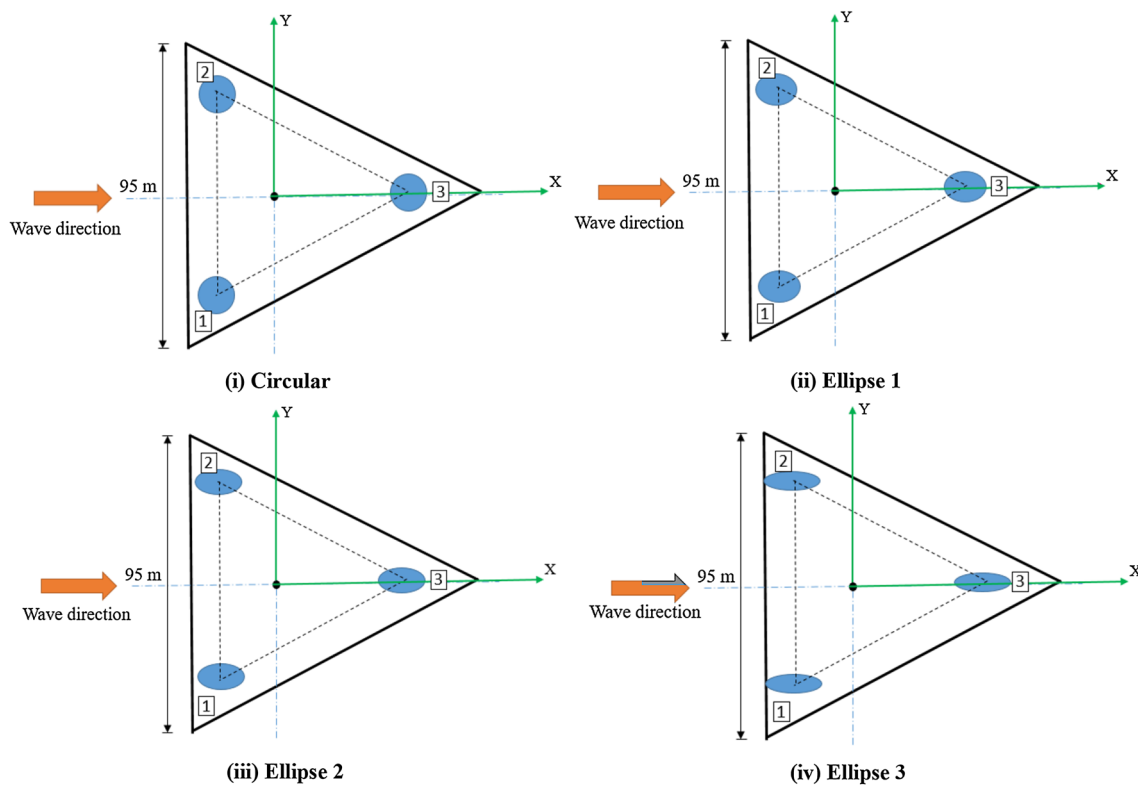
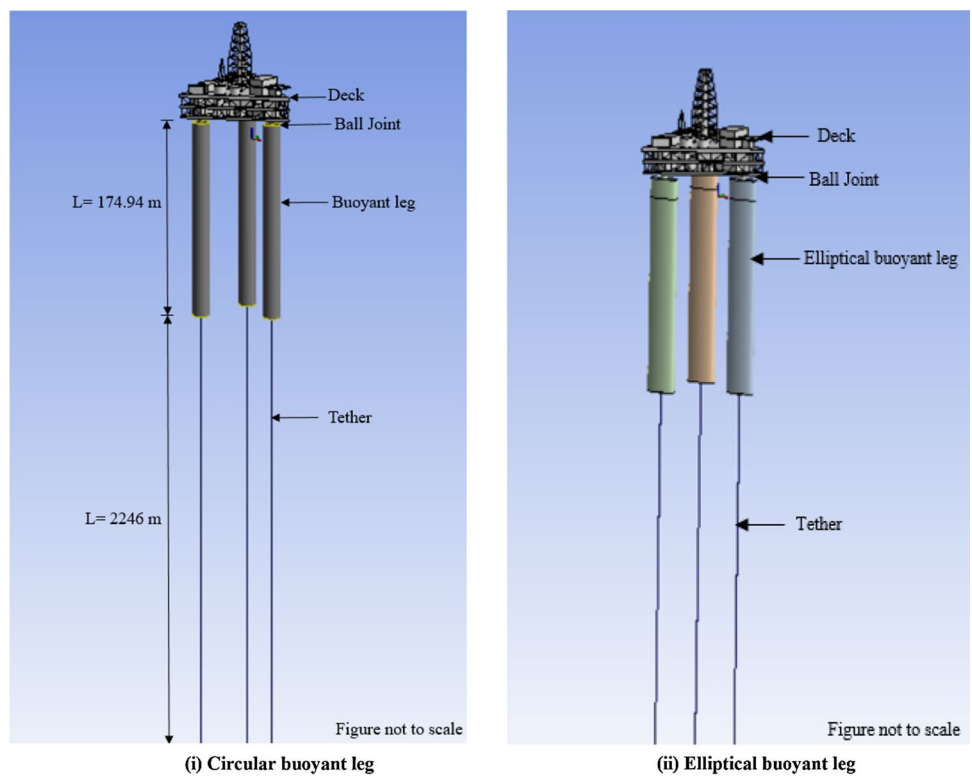


**Fig. 4** Plan view of triceratops with circular and elliptical buoyant legs

theorem is used to formulate the velocity potential within the fluid domain. The fluid pressure and the structural motion in the time domain are obtained by considering the real part of the complex potential functions. The Laplace equation describes the fluid–structure interaction, linear free surface equation, body surface conditions, seabed surface condition, and radiation condition by assuming the fluid ideal and employing linear hydrodynamic theory. The velocity potential function governed by the above set of equations is solved using the boundary integration approach. Besides, the internal lid method is employed for the source distribution approach where the fluid field is assumed to exist interior to the mean wetted body surface. More detailed analyses are carried out to assess the response behavior under regular waves.

Due to the change in the shape of the buoyant legs, there arises a significant shift in their self-weight. It, in turn, affects buoyancy and the initial pretension in each tether. These variations are listed in Table 3. It can be seen from the table that there is an increase in the total weight and a corresponding reduction in the tether force of the platform with elliptical legs compared to that of the circular legs. The weight increase in the platform with ellipse-1, ellipse-2, and ellipse-3 are about 0.3, 0.9, and 1.7%, respectively, in comparison with that of the platform with circular buoyant legs. In contrast with that of the platform with circular buoyant legs, a reduction of about 0.7, 1.9, and 3.7% in the total tether force is observed with that of the elliptical buoyant legs with eccentricities 1.5, 2, and 2.5, respectively. Reduction in tether forces aids an extended service life of tethers.

**Table 3** Weight of triceratops (MN) with different buoyant legs

Description	Circular	Ellipse 1	Ellipse 2	Ellipse 3
Weight of each buoyant leg	157.45	159.31	162.55	167.05
Total self-weight + payload	562.42	564.28	567.52	572.02
Total tether force	258.49	256.63	253.39	248.89

**Table 4** Natural frequency of tethered triceratops

Degree of freedom	Circular (rad/s)	Ellipse 1 (rad/s)	Ellipse 2 (rad/s)	Ellipse 3 (rad/s)
Surge	0.029	0.029	0.028	0.028
Sway	0.029	0.029	0.028	0.028
Heave	1.461	0.829	0.829	0.914
Roll	1.013	0.980	0.991	0.942
Pitch	1.013	0.980	0.991	0.942
Yaw	0.029	0.029	0.028	0.028

### Free oscillation studies

Free oscillation studies are carried out on the tethered triceratops to compute the natural periods in each degree of freedom; values are listed in Table 4. It is seen from the table that the natural frequency in flexible degree of freedom does not vary from that of the circular ones except in the stiff degrees of freedom like heave, roll, and pitch. Despite the differences, natural frequencies in the stiff degrees of freedom lie within the range of the dominant frequencies of waves that encounter triceratops.

### Hydrodynamic diffraction

Hydrodynamic loads on offshore structures are caused by water particle kinematics, structural motion, and wave-structure interaction. Followed by the free oscillation studies, hydrodynamic diffraction analysis is carried out with eight intermediate frequencies using a program-controlled wave frequency range to reduce the computational effort. Hydrodynamic diffraction forces acting on the buoyant legs are analyzed for varying frequencies and wave-heading angles. Significant changes are observed in the hydrodynamic characteristics of the platform with the buoyant legs of elliptical cross section. Hydrodynamic forces on a structure include Froude–Krylov force and diffraction forces. Froude–Krylov force is the first-order wave incident force, and diffraction force is the force induced by the wave disturbance due to the presence of the structure. Variations in the diffraction and Froude–Krylov forces in the buoyant leg 1 with a circular cross section are shown in Fig. 5. It is seen from the figure that the maximum forces in surge degree of freedom are observed at wave incident angles of  $-180^\circ$ ,  $0^\circ$ , and  $+180^\circ$ . It is found at a wave frequency, which is closer to half of that of the natural heave frequency under all wave incident angles. Maximum forces occur in the surge degree of freedom when the wave force acts along the positive and negative  $X$ -direction. In sway degree of freedom, peaks are observed at a frequency close to half of the natural heave frequency and wave incident angles of  $-90^\circ$  and  $+90^\circ$ . It is important to note that the maximum force developed is about 3.74 MN/m at  $0^\circ$  and  $90^\circ$  in the surge and sway degrees of

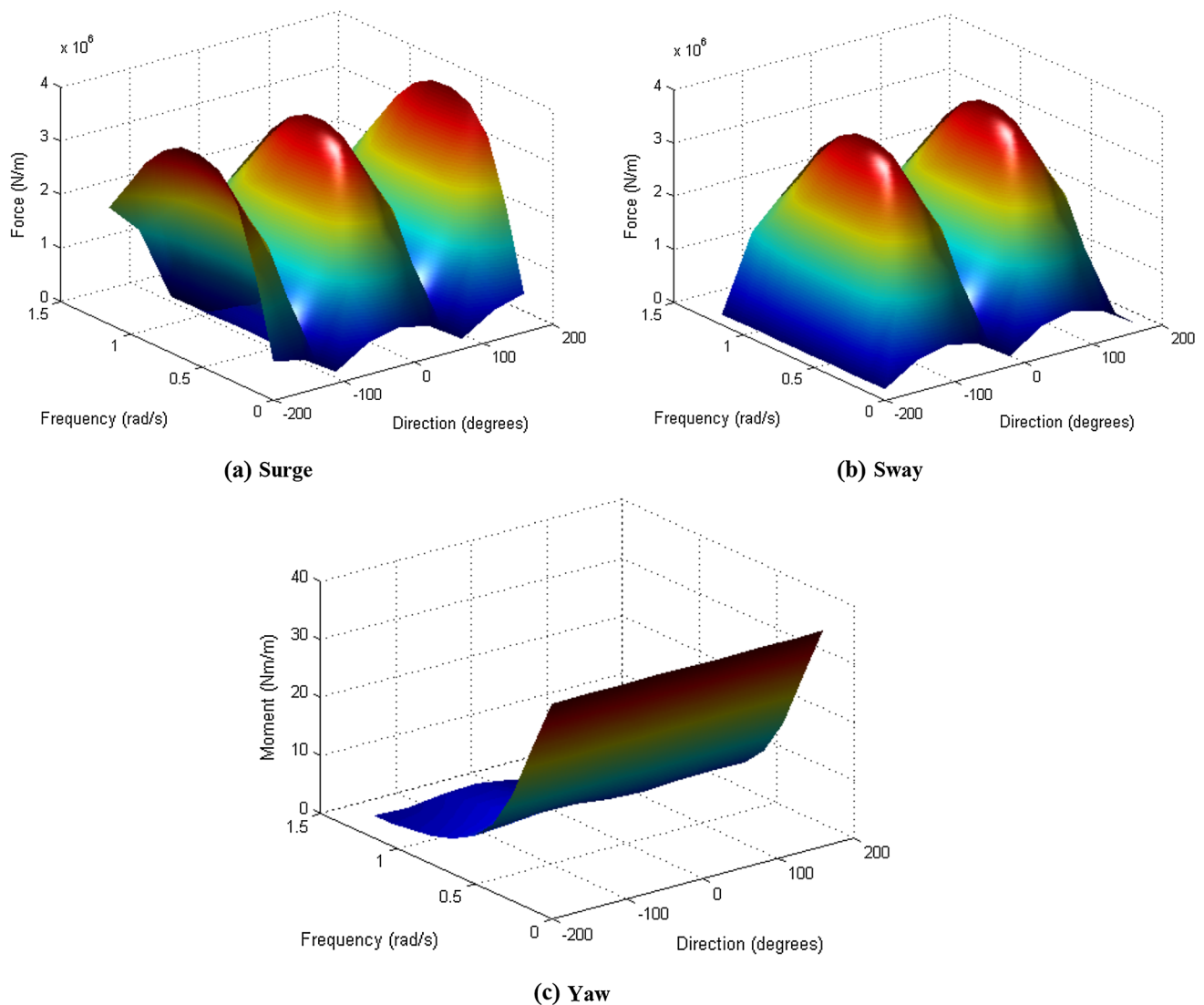


**Fig. 5** Diffraction and Froude–Krylov forces in circular buoyant leg

freedom, respectively. It is also observed that the maximum moment in the yaw degree of freedom occurs closer to the natural yaw frequency. However, no such observations are seen in the platform with circular buoyant legs.

Variations in the diffraction and Froude–Krylov forces in the buoyant leg 1 of triceratops with the elliptical cross sections are shown in Figs. 6, 7, and 8, for different shape parameters of the ellipse. It is seen from the figures that the maximum force developed in the surge degree of freedom is comparatively lesser than that of the circular buoyant leg. Significant changes are also observed in the force–frequency curves at different wave incident angles. The force pattern in ellipse-2 is similar to that of the circular buoyant leg in surge and sway degrees of freedom. Changes in the transverse vibration induced by the difference in the eccentricity of cross section lead to the

formation of significant peaks in the yaw force plots. In the case of ellipse-1, force peaks in both the surge and sway plots are observed in the neighborhood of natural heave frequency, as shown in Fig. 6. Unlike the circular buoyant leg case, several distinct peaks at various frequencies are not observed. The maximum force in surge and sway degrees of freedom are 3.24 MN and 5.07 MN at  $0^\circ$  and  $90^\circ$ , respectively. Force in the sway degree of freedom increases due to the increase in the size of the leg along the X-direction, which encounters a higher waterplane area. Besides, a shift in the maximum yaw moment also occurs from the lowest to highest frequencies with the change in the cross section of the buoyant leg. Minimum yaw moments occur in the directions parallel to the surge and sway degrees of freedom, whereas maximum moments occur at  $\pm 45^\circ$  and  $\pm 135^\circ$ .

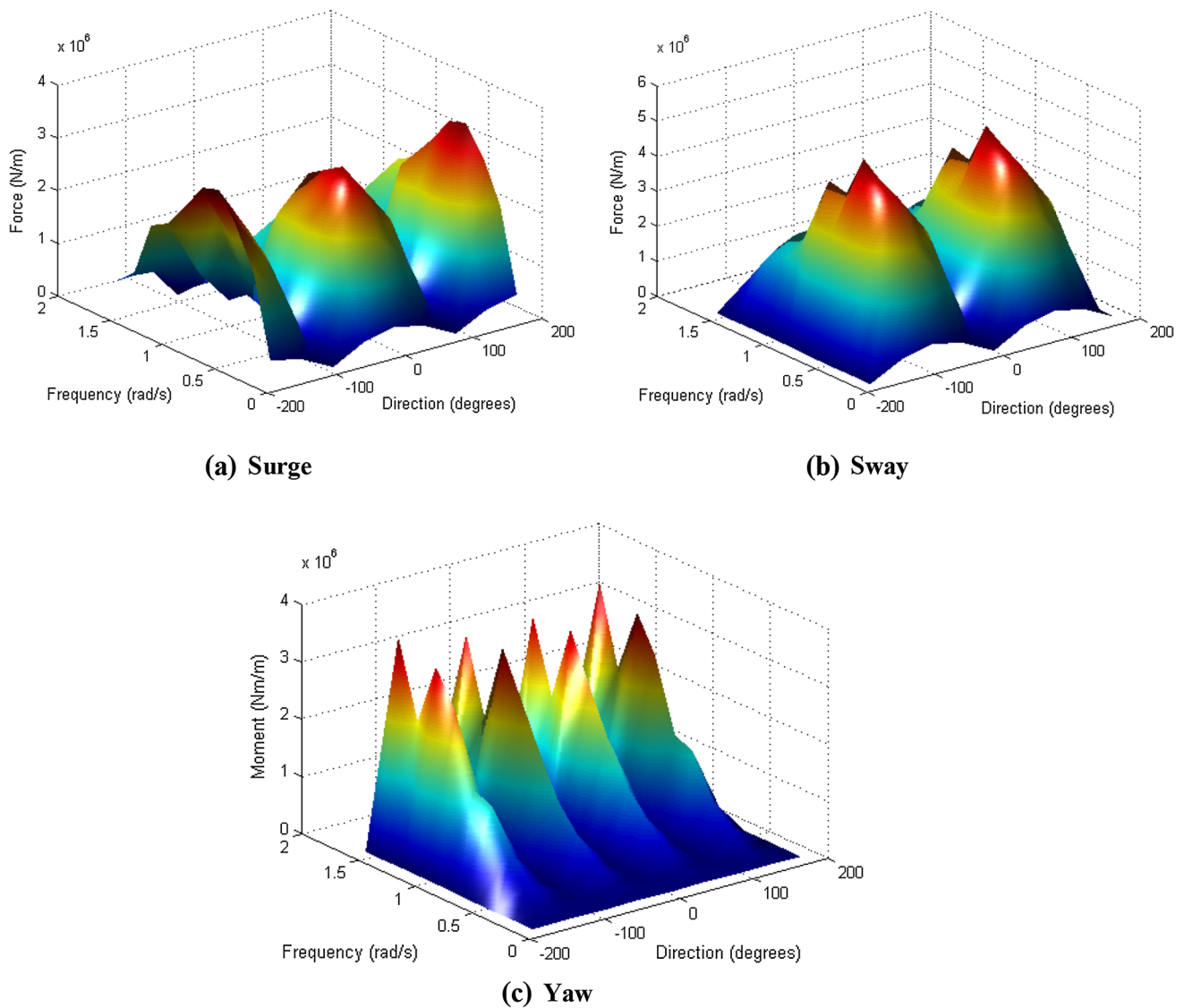


**Fig. 6** Diffraction and Froude–Krylov forces in the elliptical buoyant leg (ellipse 1)

In the case of ellipse-2 with eccentricity 2.0, the force–frequency curve is found to be similar to that of the circular buoyant legs without any significant peaks, as seen from Fig. 7. Maximum surge and sway forces of magnitude 2.66 MN and 5.91 MN occur at a frequency closer to that of natural heave frequency. A maximum yaw moment is developed at a frequency of 1.26 rad/s. Further, forces generated at the diagonal directions are also observed to be similar to ellipse-1. In the case of ellipse-3, distinct peaks are seen in the force–frequency curves of both surge and sway degrees of freedom. Maximum forces of magnitude 2.78 and 7.32 MN occur closer to that of the natural heave frequency, as shown in Fig. 8. In the yaw degree of freedom, maximum moments are developed at  $\pm 45^\circ$  and  $\pm 135^\circ$ . Variations in the force generated in yaw degree of freedom are mainly governed by the combined forces developed in the horizontal

plane along surge and sway degrees of freedom. It can be seen that the maximum forces acting on the buoyant leg in the sway degree of freedom increase with the increase in the eccentricity. Further, force variations in surge degree of freedom are nonlinear due to the combined interaction of the buoyant legs and the deck.

**Characteristics of sea state**

In the real sea state conditions, ocean waves are a combination of different frequencies and approach angles. It causes a severe limitation in the mathematical modeling of wave-forms, for which researchers use simplified theories. In the present study, regular waves are represented by the small-amplitude, linear Airy’s theory. Linear free surface condition is used in simulating the regular wave, as the wave amplitude

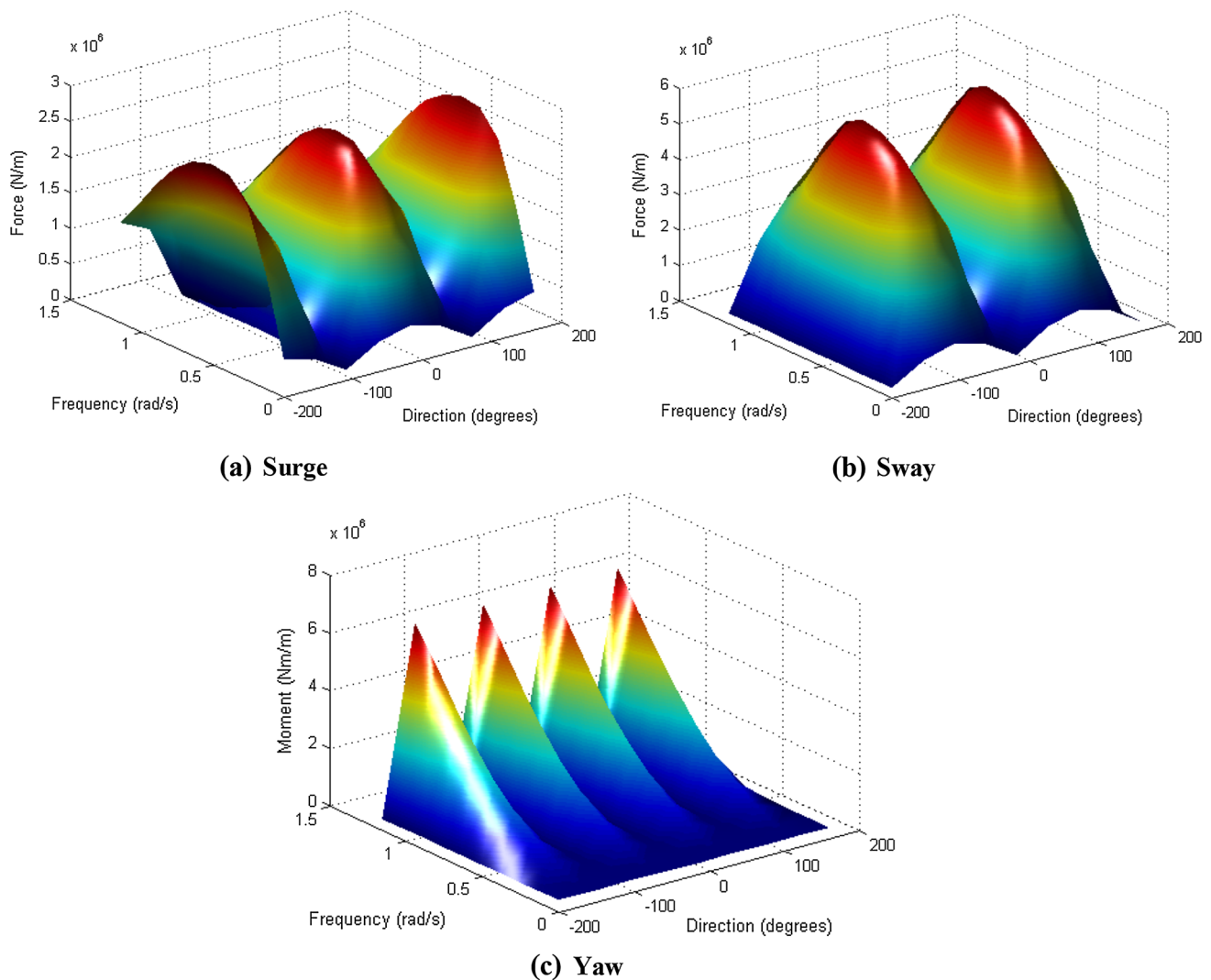


**Fig. 7** Diffraction and Froude–Krylov forces in the elliptical buoyant leg (ellipse 2)

is minimal compared to the water depth and wavelength. Various sea states considered in the present study are listed in Table 5. It is important to note that as the buoyant legs are modeled as diffraction elements, their diameter to wavelength should be maintained higher than 0.2 while selecting the sea states for the response analysis.

## Dynamic response

The time-domain analysis is carried out under different sea states to simulate the real-time motion of triceratops. Position and velocities of the deck and buoyant legs are obtained at each time step by integrating the accelerations under these environmental loads in the time domain using a two-stage predictor–corrector numerical integration scheme. The real-time motion of the structure is simulated under the action of

regular waves, and the nonlinear Froude–Krylov and hydrostatic forces are estimated under an instantaneous incident wave surface. The analysis is carried out through the calculation of nonlinear forces on the meshed panels of the structure along with the instantaneous values of cable tension at each time step during the simulation. The accelerations are then determined by applying the calculated forces to the structure through a set of nonlinear equations of motion. Wave loads are applied at an incident wave angle, as shown in Fig. 4. Dynamic response of deck, buoyant legs, and tethers are examined in detail.

## Deck response under different sea states

The total response of deck in different degrees of freedom at zero-degree incident wave angle is given in Table 6. It is observed that the response increases with the increase in



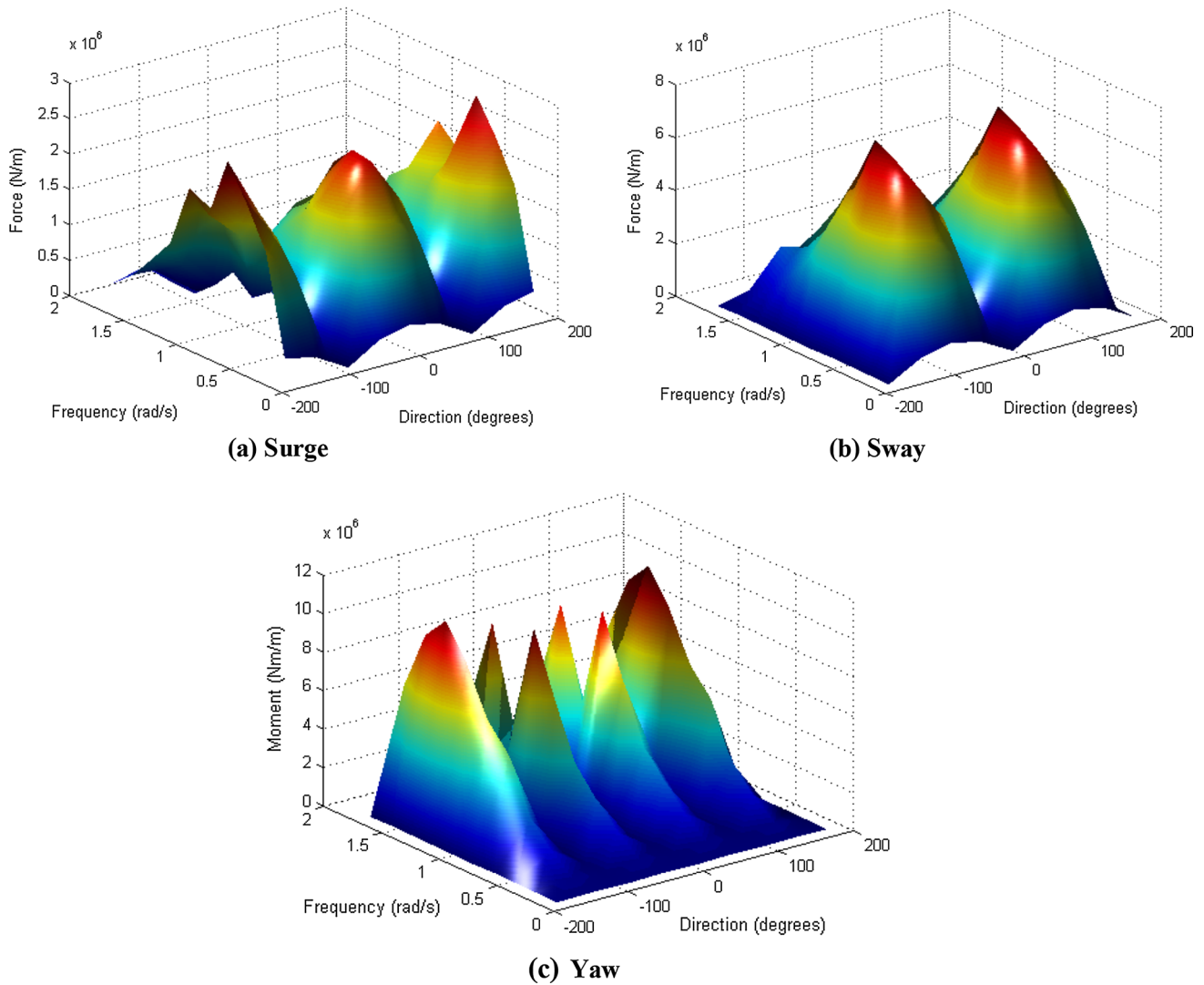


Fig. 8 Diffraction and Froude–Krylov forces in the elliptical buoyant leg (ellipse 3)

Table 5 Characteristics of sea states

Sea state description	Douglas sea state	Wave height $H$ (m)	Wave period $T$ (s)	Wind speed (m/s)
Rough	4	2.0	5.0	10
High	6	4.0	5.0	20

the roughness of the sea state. It is further seen that the total surge response of the deck under ellipse-1 increases by about 26% in comparison with that of the platform with circular buoyant legs. It is important to note that the increase in the deck response decreases with the increase in the eccentricity of the shape of the elliptical buoyant legs. Under circular buoyant legs, sway response of the deck is about 4.70% of that of the surge while sway response is lesser when

Table 6 Deck response under different sea states

Sea state	Degree of freedom	Circular	Ellipse 1	Ellipse 2	Ellipse 3
Rough	Surge (m)	0.4047	0.5098	0.4296	0.4067
	Sway (m)	0.0192	0.1434	0.0348	0.1537
	Heave (m)	0.0012	0.0012	0.0011	0.0011
	Roll ( $^\circ$ )	0.0035	0.0031	0.0027	0.0028
	Pitch ( $^\circ$ )	0.0037	0.0038	0.0036	0.0034
High	Yaw ( $^\circ$ )	0.0253	0.3688	0.0815	0.0293
	Surge (m)	0.8471	1.6684	0.8189	0.9197
	Sway (m)	0.0778	1.0732	0.0514	0.5438
	Heave (m)	0.0015	0.0014	0.0014	0.0013
	Roll ( $^\circ$ )	0.0024	0.0038	0.0021	0.0035
	Pitch ( $^\circ$ )	0.0055	0.0048	0.0051	0.0044
	Yaw ( $^\circ$ )	0.0711	1.9830	0.1178	0.9904

compared to the surge response only in case of ellipse-2; transverse vibration is also lower in this case. Transverse vibration is found to be higher in the case of ellipse-3, where the sway response is about 38% of that of the surge. Heave, roll, pitch, and yaw responses of the deck decrease with the increase in the eccentricity of the shape of elliptical buoyant legs. In high sea state, surge response of the deck in case of ellipse-2 is marginally lesser than that of the circular ones, whereas it is higher for the other two cases. Transverse vibration is also comparatively lower in the case of ellipse-2.

Further, sway response is only about 6.3% of that of the surge in the case of ellipse-2, whereas it is about 9% in the platform with circular buoyant legs. Reduced heave, roll, and pitch responses are also observed in the case of ellipse-2 in comparison with the circular ones. However, there is an increase in the yaw response by about 66%. It is therefore clear that the shape of the buoyant legs does not influence the stiff degrees of freedom; only flexible degrees of freedom such as surge, sway, and yaw show more considerable variations with the change in the eccentricity of the buoyant legs. It is also important to note that offshore platforms in ultra-deepwaters, in general, and triceratops, in particular,

are designed to remain flexible in these degrees of freedom. Out of all the cases under consideration, ellipse-2 with eccentricity 2.0 is found to be advantageous with a reduced deck response. Besides, heave response is only about 0.3% and 0.2% even under rough and high sea states, respectively. Phase plots of different cases in the surge degree of freedom are shown in Fig. 9. These plots also highlight the increased stability of elliptical-shaped buoyant legs (ellipse-2 configuration). It shows the suitability of the platform with elliptical buoyant legs in ultra-deepwater conditions.

### Buoyant leg response

The response of a single buoyant leg is examined in detail; the response of buoyant leg-1 under different sea states is given in Table 7. It is seen from the table that under rough sea state, surge response in all cases of the elliptical sections is higher than that of the circular case. Response in the ellipse-3 section is lesser than that of other sections, but still about 2.5% greater than that of the circular ones. Though ball joints are designed in such a way to transfer only translational motion between the deck and the buoyant

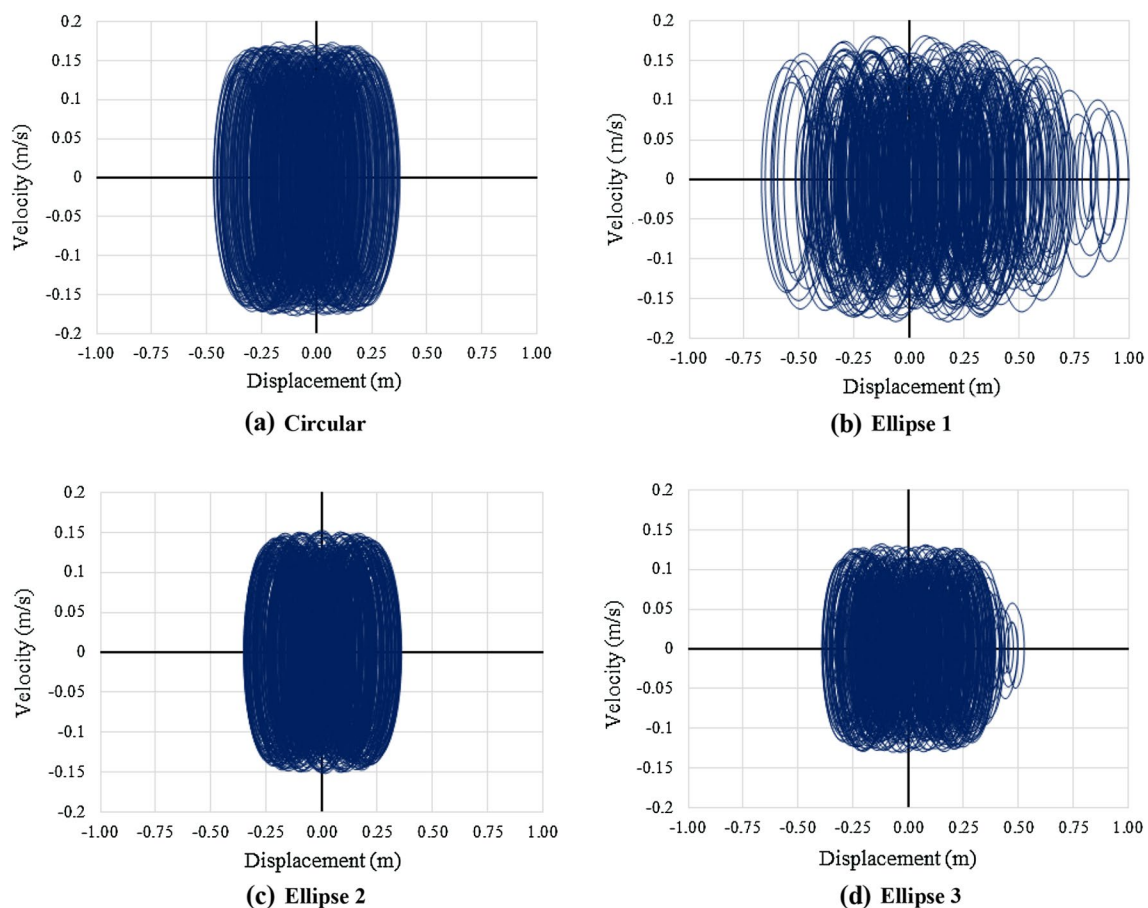


**Fig. 9** Phase plots of the deck under surge degree of freedom

**Table 7** Buoyant leg response under different sea states

Sea state	Degree of freedom	Circular	Ellipse 1	Ellipse 2	Ellipse 3
Rough	Surge (m)	0.2910	0.3660	0.3438	0.2983
	Sway (m)	0.0284	0.2885	0.0805	0.1575
	Heave (m)	0.0028	0.0027	0.0029	0.0027
	Roll (°)	0.0056	0.0800	0.0050	0.0086
	Pitch (°)	0.1290	0.1272	0.0883	0.0969
	Yaw (°)	3.8035	1.8000	0.9267	0.8999
High	Surge (m)	0.6125	1.3886	0.6054	0.8196
	Sway (m)	0.0205	1.9791	0.1022	0.9207
	Heave (m)	0.0038	0.0036	0.0034	0.0033
	Roll (°)	0.0443	0.1887	0.0041	0.0735
	Pitch (°)	0.2627	0.2662	0.1808	0.1977
	Yaw (°)	3.0430	6.8080	2.4439	4.3427

legs, the coupling between various degrees of freedom invokes a rotational response of the deck as well. Surge and heave degrees of freedom are coupled due to the compliancy while the surge is coupled with pitch due to the shift in the point of action of wave load from that of the center of gravity of the buoyant legs. These coupling characteristics affect the total magnitude of responses in different degrees of freedom while making it further complicated. Similar to that of the deck response, transverse vibration is found to be lesser in the elliptical cross section of eccentricity 2.0. The sway response under this case is about 23% of that of the surge. Comparatively, a lower yaw response is observed in the ellipse cases than that of the circular ones; yaw response in case of ellipse-2 is only about 24% of that of the circular ones.

In high sea state, surge response is lesser in the case of ellipse-2 in comparison to that of the circular ones. Reduced pitch response is also observed in the elliptical buoyant legs under both rough and high sea state conditions. In high sea

state, pitch response of the deck is only about 3.0% of that of the elliptical buoyant leg, proving the effectiveness of the ball joints in restraining the transfer of rotational motion from buoyant legs to the deck. However, a total restraint cannot be achieved due to the differential heave motion in the buoyant legs.

**Total force in the buoyant legs**

The shape of the cross section influences total forces developed on the buoyant legs. Forces generated under different sea states are given in Table 8. It is seen from the table that the maximum force along the X-axis is observed in the case of ellipse-3 and ellipse-1 under rough and high sea states, respectively. By comparing the cases of the elliptical buoyant legs, it is seen that the total forces developed along Y-axis are lesser in the case of the ellipse-2 case under both the sea states. It is also observed that the total force in the horizontal plane is maximum in the elliptical cases. At the same time, it is found to be the maximum with circular buoyant legs in the vertical plane. Due to a reduced drag in a circular configuration, the total moment about the x-axis is lesser in the circular buoyant legs in comparison with that of the elliptical buoyant legs. Significant changes in the moment about Y-axis are not observed among the elliptical buoyant legs. Total force–time history in the different degrees of freedom under high sea state is shown in Fig. 10.

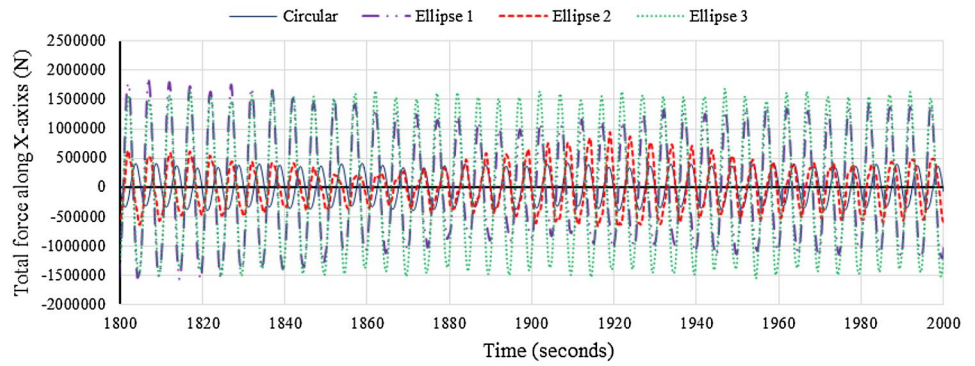
**Tether tension variation**

The initial tension of the tethers is changed according to the change in the weight of the buoyant legs. It is done to maintain the same draft level in all cases. The motion of triceratops under wave action alters the initial tension in the tethers used for position-restraining the buoyant legs; these variations under different cases under both rough and high sea states are listed in Table 9. It is seen from the

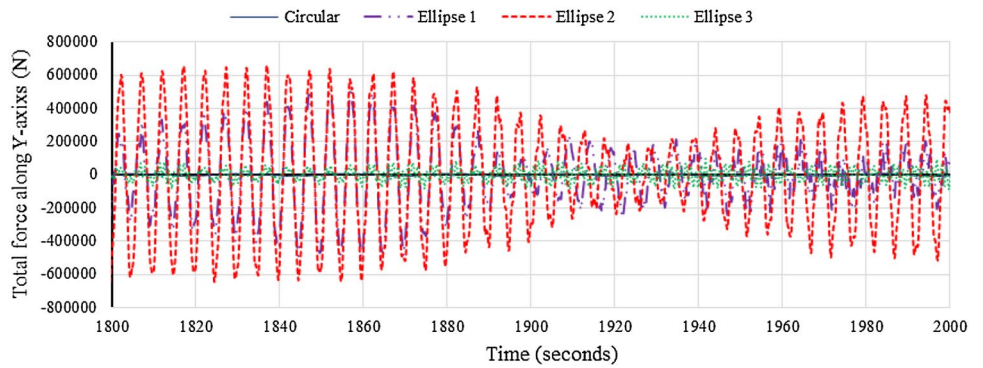
**Table 8** Total force in the buoyant leg under different sea states

Sea state	Degree of freedom	Circular	Ellipse 1	Ellipse 2	Ellipse 3
Rough	Surge (kN)	408.32	1926.88	1597.879	1393.178
	Sway (kN)	4.27	546.22	174.418	180.573
	Heave (kN)	1265.29	418.34	362.096	328.36
	Roll (kNm)	2878.95	11,581.09	9798.08	10,386.43
	Pitch (kNm)	56,975.78	10,799.11	10,183.17	10,108.35
	Yaw (kNm)	10.91	798.63	717.816	556.578
High	Surge (kN)	523.71	3807.25	3247.56	2806.33
	Sway (kN)	17.76	1164.98	208.31	1312.93
	Heave (kN)	1337.52	416.92	464.96	403.11
	Roll (kNm)	2412.70	14,868.93	10,605.42	10,492.38
	Pitch (kNm)	11,577.86	11,308.86	11,669.43	10,168.39
	Yaw (kNm)	138.16	3912.09	3278.16	5907.57

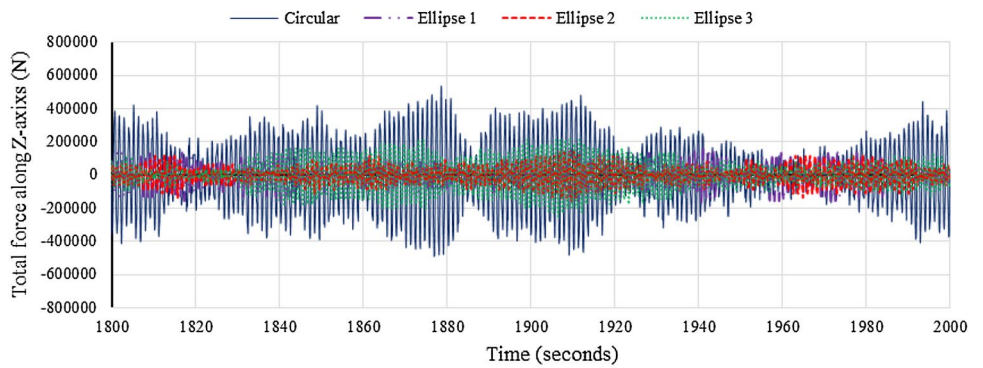
**Fig. 10** Total force–time history under high sea state in buoyant leg 1



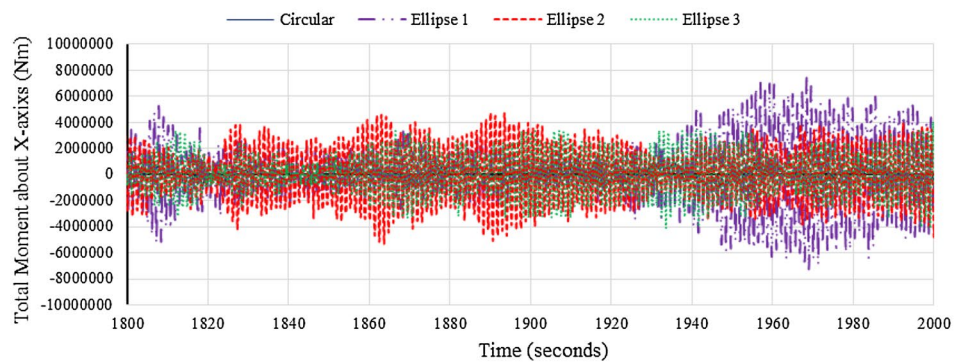
**(a) Total force along X-axis**



**(b) Total force along Y-axis**



**(c) Total force along Z-axis**



**(d) Total moment about X-axis**

Fig. 10 (continued)

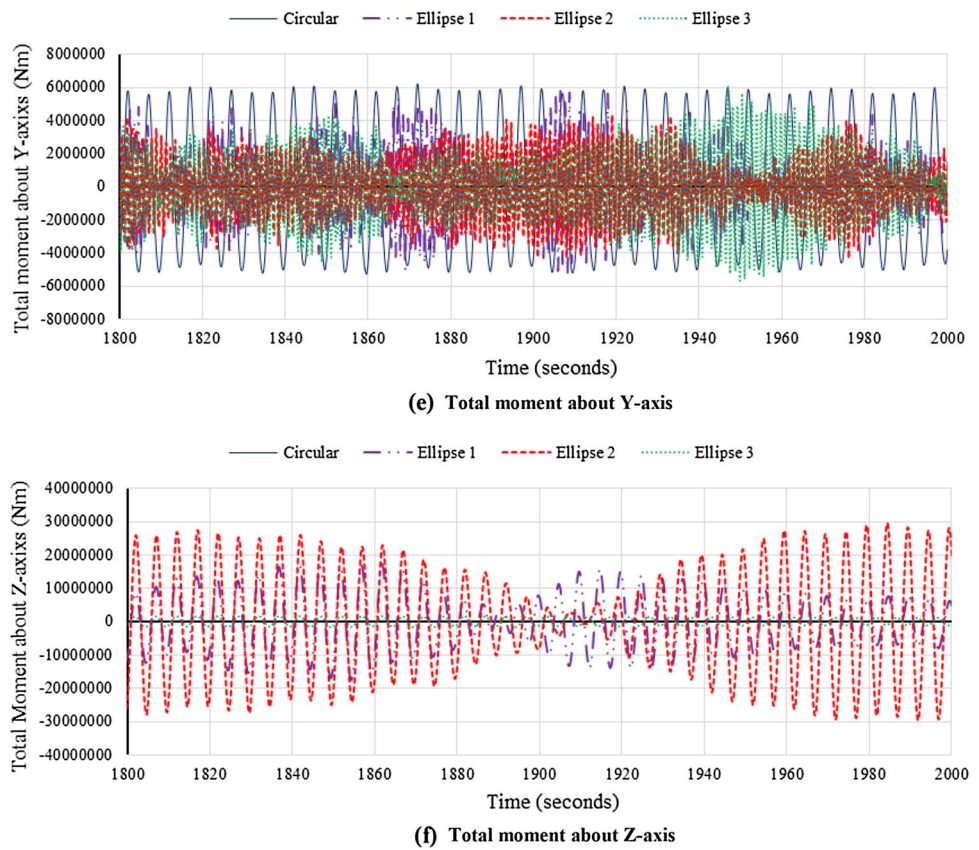


Table 9 Tether tension variations

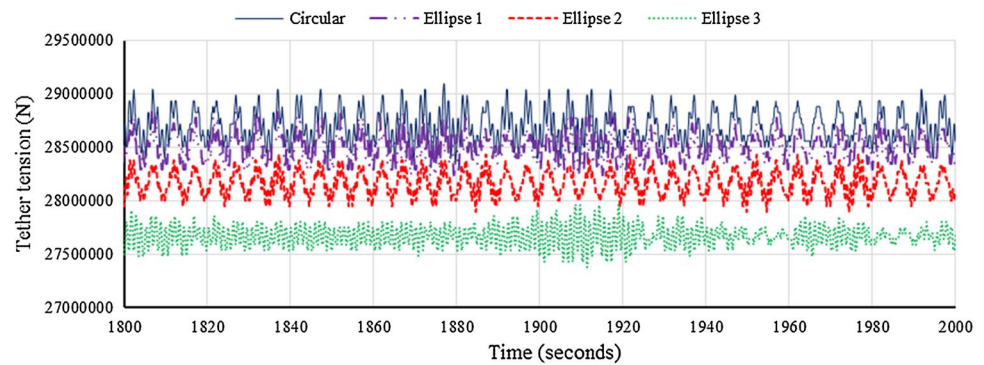
Sea state	Tether tension	Circular	Ellipse 1	Ellipse 2	Ellipse 3
Rough	Maximum (MN)	29.04	28.83	28.42	27.97
	Minimum (MN)	28.40	28.19	27.83	27.38
	Tether tension variation (%)	2.20	2.20	2.10	2.10
High	Maximum (MN)	29.15	28.89	28.48	28.02
	Minimum (MN)	28.29	28.08	27.84	27.32
	Tether tension variation (%)	3.00	2.80	2.30	2.50

table that the initial pretension in a single tether of circular, ellipse-1, ellipse-2, and ellipse-3 legs is 28.72, 28.51, 28.15, and 27.65 MN respectively. Smaller changes in the initial pretension are due to the difference in the total weight of the buoyant legs with different cross sections. Further, the tension variation increases with the increase in the roughness of the sea state under all cases. In the rough sea state, there is no significant difference in the tension variation to the changes in the cross section of the buoyant legs. However, in high sea state, a maximum tension variation is observed in the circular legs. In contrast, a minimum difference is seen in the elliptical legs with eccentricity 2.0, which is an added advantage to the cross section of the ellipse-2 configuration. Tether tension response of different buoyant leg cases under high sea state is shown in Fig. 11.

### Conclusions

New generation offshore platforms are being developed in recent years to overcome the operational challenges under adverse environmental conditions. Offshore triceratops is one such steel platforms, which are recently being investigated for their suitability in ultra-deepwater exploration. The present study examined the dynamic response of triceratops with elliptical buoyant legs under different sea states. Free oscillation studies showed that a change in the shape of the cross section of buoyant legs influences the natural frequency in stiff degrees of freedom. Even under the unidirectional waves, diffraction, and the Froude–Krylov forces, acting along with the sway degree of freedom increases with an increase in the eccentricity of the shape

**Fig. 11** Tether tension variation in buoyant leg-1 under high sea state



of elliptical sections. Further, the hydrodynamic response under different sea states showed that the elliptical buoyant leg with eccentricity 2.0 is comparatively advantageous than that of other cross sections. It showed a reduced deck response with increased stability in different degrees of freedom. Also, a reduced tether tension variation in the case of ellipse-2 adds to its advantage.

## References

- CEN EN, EN (2006) Hot finished hollow structural sections of non-alloy and fine grain steels-part 2: tolerances dimensions and sectional properties. Comité Européen de Normalisation Brussels, Belgium
- Chandrasekaran S, Mayanak S (2017) Dynamic analyses of stiffened triceratops under regular waves: experimental investigations. *Ships Offshore Struct* 12(5):697–705. <https://doi.org/10.1080/17445302.2016.1200957>
- Chandrasekaran S, Nagavinothini R (2018) Dynamic analyses and preliminary design of offshore triceratops in ultra-deep waters. *Innov Infrastruct Solut* 3(1):16. <https://doi.org/10.1007/s41062-017-0124-1>
- Chandrasekaran S, Nagavinothini R (2018) Tether analyses of offshore triceratops under the wind, wave, and current. *Marine Syst Ocean Technol* 13(1):34–42. <https://doi.org/10.1007/s40868-018-0043-9>
- Chandrasekaran S, Nagavinothini R (2019) Tether analyses of offshore triceratops under ice force due to continuous crushing. *Innov Infrastruct Solut* 4(1):25. <https://doi.org/10.1007/s41062-019-0212-5>
- Chatjigeorgiou IK (2011) Three-dimensional wave scattering by arrays of elliptical and circular cylinders. *Ocean Eng* 38(13):1480–1494. <https://doi.org/10.1016/j.oceaneng.2011.07.001>
- Chatjigeorgiou IK, Katsardi V (2018) Hydrodynamics and near trapping effects in arrays of multiple elliptical cylinders in waves. *Ocean Eng* 157:121–139. <https://doi.org/10.1016/j.oceaneng.2018.03.045>
- Chatjigeorgiou IK, Mavrakos SA (2010) An analytical approach for the solution of the hydrodynamic diffraction by arrays of elliptical cylinders. *Appl Ocean Res* 32(2):242–251. <https://doi.org/10.1016/j.apor.2009.11.004>
- Liapis S, Bhat S, Caracostis C, Webb C, Lohr C (2010) Global performance of the Perdido spar in waves, wind and current: Numerical predictions and comparison with experiments. In: ASME 2010 29th International conference on ocean, offshore and arctic engineering, pp 863–873. American Society of Mechanical Engineers Digital Collection. <https://doi.org/10.1115/OMAE2010-21116>
- Nagavinothini R, Chandrasekaran S (2019) Dynamic analyses of offshore triceratops in ultra-deep waters under the wind, wave, and current. *Structures* 20:279–289. <https://doi.org/10.1016/j.istruc.2019.04.009>
- Silvestre N (2008) Buckling behavior of elliptical cylindrical shells and tubes under compression. *Int J Solids Struct* 45(16):4427–4447. <https://doi.org/10.1016/j.ijsolstr.2008.03.019>
- Srinivasan C, Nagavinothini R (2019) Ice-induced response of offshore triceratops. *Ocean Eng* 180:71–96. <https://doi.org/10.1016/j.oceaneng.2019.03.063>
- Tennyson RC, Booton M, Caswell RD (1971) Buckling of imperfect elliptical cylindrical shells under axial compression. *AIAA J* 9(2):250–255. <https://doi.org/10.2514/3.6159>
- Veritas DN (2010) Buckling strength of shells, recommended practice DNV-RP-C202. Det. Nor. Ver. Class. AS Veritasveien 1
- Wang P, Zhao M, Du X, Liu J (2019) Analytical solution for the short-crested wave diffraction by an elliptical cylinder. *Eur J Mech B Fluids* 74:399–409. <https://doi.org/10.1016/j.euromechflu.2018.10.006>
- White CN, Copple RW, Capanoglu C (2005) Triceratops: an effective platform for developing oil and gas fields in deep and ultra-deepwater. In: The fifteenth international offshore and polar engineering conference. International Society of Offshore and Polar Engineers
- Williams AN (1985) Wave diffraction by elliptical breakwaters in shallow water. *Ocean Eng* 12(1):25–43. [https://doi.org/10.1016/0029-8018\(85\)90009-5](https://doi.org/10.1016/0029-8018(85)90009-5)
- Williams AN, Darwiche MK (1988) Three-dimensional wave scattering by elliptical breakwaters. *Ocean Eng* 15(2):103–118. [https://doi.org/10.1016/0029-8018\(88\)90022-4](https://doi.org/10.1016/0029-8018(88)90022-4)